Pion elastic scattering and double charge exchange on heavy nuclei in the generalized seniority model

H. C. Wu
Departamento de Fisica, Universidad de Antioquia, Medellin, Colombia

W. R. Gibbs
Physics Department, New Mexico State University, Las Cruces, New Mexico 88003
(Received 7 February 2000; published 18 September 2000)

The π-nucleus optical potential is extended to open shell nuclei by employing the generalized seniority model and partial Pauli blocking. The calculated optical potentials are fit to π-nucleus elastic scattering data on ^{90}Zr and ^{208}Pb at resonance as well as low energies. The ranges of the πN interaction are determined by a best fit to experimental data. The angular distribution at 48 MeV pion lab energy and energy dependence of the double charge exchange cross section on Te isotopes are calculated. The existing experimental data are reproduced by using the ranges in the vicinity of the averaged ranges of ^{90}Zr and ^{208}Pb determined in fitting elastic-scattering data.

PACS number(s): 13.75.Gx, 25.80.Gn, 24.10.Ht, 21.60.Cs

I. INTRODUCTION

The pion-nucleus double charge exchange (DCX) reaction is a unique tool for revealing nucleon-nucleon correlations in nuclei [1,2]. However, the existing studies of the DCX reaction are mainly on light nuclei. Since for medium and heavy nuclei the nucleon-nucleon correlation also plays a very important role, one can hope that the study of DCX reactions may bring about new opportunities to deepen our understanding of the structure of these nuclei.

There exist several theoretical studies of the DCX reaction on Te isotopes [3,4], but they are in a less quantitative stage, compared to the study of DCX in the light nuclei. In [3] the quasi-particle-random-phase approximation (pnQRPA) is applied to account for nucleon-nucleon correlations in nuclei, and the authors are able to explain the DCX rates by adjusting the particle-particle interaction strengths [3]. While pnQRPA has gained some success in the study of double beta decay, one needs to be more careful when the method is applied to the study of the DCX reaction, since a prominent feature of the pnQRPA is the nonconservation of particle numbers. The DCX reaction is a complex multistage process, which involves two charge exchanges, the propagation of intermediate π^0 and the scattering of incoming and outgoing pions. Pion scattering from the remainder of the nucleons is crucial in calculating the DCX cross section and requires a realistic π-nucleus optical potential [5]. Therefore, it seems more appropriate to employ a nuclear model with well-defined nucleon numbers, from which one can derive a realistic π-nucleus optical potential. In this regard, the shell model appears more advantageous, as it provides a nuclear wave function that conserves the number of nucleons. However, the huge configuration space presents a formidable obstacle. As is done in the nuclear structure study, one often employs simplifications of the shell model in dealing with the nuclear wave function. The generalized seniority model is one such simplification, and it has been applied [4] to the DCX reaction. It was shown in that study that nuclear structure, while relatively unimportant in the double isobaric analog state (DIAS) transition, plays an important role in the ground-state (g.s.) transition. However, that investigation is only schematic, since it is based on the plane-wave limit.

In the present work we study the DCX reaction on Te isotopes based on the generalized seniority model together with the most important ''realistic'' elements of the DCX reaction: the nuclear density distribution, and distortions in the incoming and outgoing π waves and the π^0 propagation.

The paper is organized as follows: Sec. II discusses the calculation of the π-nucleus optical potential with Pauli blocking in an open shell nucleus. In Sec. III the calculated optical potential is fine tuned by fitting to elastic scattering data on ^{90}Zr and ^{208}Pb. The DCX reaction on Te isotopes, which is the primary aim of this work, is discussed and calculated in Sec. IV. Section V contains the conclusions and discussion.

II. CALCULATION OF π-NUCLEUS OPTICAL POTENTIAL FOR OPEN SHELL NUCLEI

To investigate the π-nucleus optical potential a formalism was proposed in [6,7] and applied to closed shell nuclei. However, for open shell nuclei the nucleon-nucleon correlation makes all the single-particle orbits in the valence shell partially filled, and the Pauli blocking, which has been shown important in the calculation of optical potential [7], becomes complicated (for convenience, hereafter, we call this blocking in a partially filled shell ''partial Pauli blocking''). In this work we modify the formalism of Refs. [6,7] to incorporate the partial Pauli blocking by using the scheme of the generalized seniority model.

The generalized seniority model is a good approximation when the nucleus has valence nucleons (or protons) only [8]. In this case the ground state is well approximated by a condensate of angular momentum zero (monopole) pair, where the internal structure of these monopole pairs is mass independent. For the heavier nuclei investigated in this paper, such as the isotopes of Te, we will use a less restrictive

TABLE I. Pair structure coefficients of ^{130}Te and ^{130}Xe in the generalized seniority scheme.

j	7/2	5/2	3/2	1/2	11/2
$\alpha_{\pi j}$	1.9403	0.8561	0.4510	0.3937	−0.3792
$\gamma_{\pi j}$	0.2015	0.0392	0.0109	0.0083	0.0077
$\alpha_{\nu j}$	1.3390	1.5898	0.3694	0.5418	−0.4719
$\gamma_{\nu j}$	0.9583	0.9698	0.5932	0.7736	0.7162

interpretation in which the ground state is still described as a condensate of monopole pairs but where the internal structure is taken to be mass dependent and determined from a ground-state energy minimization procedure, as is done in Ref. [9]. It has been shown that this less restrictive general seniority scheme yields an excellent approximation to the results of a complete shell-model calculation for a series of medium and heavy nuclei [9]. In the following we will use this extension of the generalized seniority scheme.

In the extension of the generalized seniority scheme used in this work, the ground state is written as

$$|\text{g.s.}\rangle = |S_\pi^{N_\pi} S_\nu^{N_\nu}\rangle, \tag{2.1}$$

where

$$S_\rho^\dagger = \sum_j \alpha_{\rho j} S_\rho^\dagger(j); \quad S_\rho^\dagger(j) = \sqrt{\frac{\Omega_j}{2}} (c_{j,\rho}^\dagger c_{j,\rho}^\dagger)^{(0)}; \quad (\rho = \pi, \nu). \tag{2.2}$$

The pair-structure coefficients, $\alpha_{\rho j}$, are determined by a variational calculation to minimize the energy of the ground state and are thus mass dependent. As an example, in Table I we list the pair structure coefficients (taken from Ref. [9]) for ^{130}Te and ^{130}Xe. In the generalized seniority scheme the particle number conservation is strictly obeyed.

Following Refs. [6,7], the optical potential can be expressed as

$$\langle \boldsymbol{k}' | V_{\text{opt}}(E) | \boldsymbol{k} \rangle = \frac{A-1}{A} \sum_i \langle \boldsymbol{k}' \phi_i | t_{\pi i}(E) | \boldsymbol{k} \phi_i \rangle, \tag{2.3}$$

where $\boldsymbol{k}$ and $\boldsymbol{k}'$ are the initial and final momenta of pion, A is the number of nucleons, ϕ_i is the bound state of the ith nucleon, and the operator $t_{\pi i}(E)$ is T matrix of the scattering of the π from the ith nucleon ([6]). For heavy nuclei the factor $(A-1)/A$ is almost equal to one, thus it can be neglected.

For open shell nuclei it is more convenient to work in the second quantized formalism, in which the above optical potential (for closed shell nuclei) can be expressed by the following operator:

$$\hat{V} = \sum_{j,m} t_{jj} a_{jm}^\dagger a_{jm}, \quad \text{where} \quad t_{jj} = \langle \boldsymbol{k}' \phi_j | t_{\pi N}(E) | \boldsymbol{k} \phi_j \rangle, \tag{2.4}$$

where j represents the single-particle orbit while other notations are the same as in above. The extension to open shell nuclei is trivial:

$$\hat{V} = \sum_{j_2 j_1, m} t_{j_2 j_1} a_{j_2 m}^\dagger a_{j_1 m},$$

where

$$t_{j_2 j_1} = \langle \boldsymbol{k}' \phi_{j_2} | t_{\pi \text{N}}(E) | \boldsymbol{k} \phi_{j_1} \rangle, \tag{2.5}$$

which is different from Eq. (2.4) by including the off-diagonal matrix elements ($j_1 \neq j_2$), since all the single-particle orbits in the valence shell are partially occupied.

The optical potential can be taken as the expectation of the operator $\hat{V}$

$$\langle \boldsymbol{k}' | V_{\text{opt}}(E) | \boldsymbol{k} \rangle = \langle \text{g.s.} | \hat{V} | \text{g.s.} \rangle, \tag{2.6}$$

where $|\text{g.s.}\rangle$ is the ground state in the generalized seniority scheme. It is obvious that, for closed shell nuclei this formalism is identical to that in Refs. [6,7], however, it also works for open shell nuclei.

Since off-diagonal terms in Eq. (2.5) break the seniority zero pairs, $S_\pi^\dagger$ and $S_\nu^\dagger$ [Eq. (2.2)], their contribution to optical potential in Eq. (2.6) will vanish and only diagonal terms are relevant. Therefore, we can have

$$\langle \boldsymbol{k}' | V_{\text{opt}}(E) | \boldsymbol{k} \rangle = \langle S_\nu^{N_\nu} S_\pi^{N_\pi} | \hat{V} | S_\nu^{N_\nu} S_\pi^{N_\pi} \rangle = \sum_j \langle \boldsymbol{k}' \phi_j | t_{\pi \text{N}}(E) | \boldsymbol{k} \phi_j \rangle (2j+1) \gamma_j, \tag{2.7}$$

where

$$\gamma_j = \sum_m \langle S_\nu^{N_\nu} S_\pi^{N_\pi} | a_{jm}^\dagger a_{jm} | S_\nu^{N_\nu} S_\pi^{N_\pi} \rangle, \tag{2.8}$$

which can be calculated by a pair-operator expansion technique of [10], and the results are listed in Table I.

Next we consider the Pauli blocking for the partially filled orbits. Since the coefficient γ_j is the occupation probability of the single-particle orbit j, it seems reasonable to assume that the effectiveness of Pauli blocking is proportional to γ_j, thus, the Pauli-blocked T matrix, t_{jj}, can be taken as the following combination:

$$t_{jj} = \gamma_j \langle \boldsymbol{k}' \phi_j | v_{\pi N}(E) | \boldsymbol{k} \phi_j \rangle + (1-\gamma_j) \langle \boldsymbol{k}' \phi_j | t_{\pi N}(E) | \boldsymbol{k} \phi_j \rangle, \tag{2.9}$$

i.e., the πN T-matrix element with the partial Pauli blocking, t_{jj}, takes the value of the πN potential when the orbit is blocked, and it takes the value of the πN T matrix when the orbit is not blocked. We calculate the optical potential of ^{90}Zr, ^{208}Pb, and ^{128,130}Te, and the results are to be tested in elastic scattering and double charge exchange reaction, which are discussed in the following two sections.

III. ELASTIC SCATTERING ON MEDIUM AND HEAVY NUCLEI

Due to the crucial importance of the π wave distortion in the DCX reaction [5], we shall test the validity of the calculated optical potential by fitting the π-nucleus elastic scattering on heavy nuclei. A recent work [11] has shown that the calculated optical potential can reproduce well the elastic scattering on light nuclei such as ^{14}C, ^{16}O, and ^{40}Ca. To serve the purpose of this work the ideal test objects would be the isotopes of Te. However, restricted by the availability of experimental data, we will instead test the optical potential calculation by fitting the elastic scattering on ^{208}Pb and ^{90}Zr [12–14]. The fitting will be conducted on low energies 30, 40, and 50 MeV as well as on the resonance region ($E_\pi = 162$ MeV).

The optical model for the pionic elastic scattering and the fitting strategy are described in Ref. [11] and references therein. Here we only note the following:

(1) In calculating the π-nucleus interaction six ranges α_i are employed (as in Ref. [11]), which correspond to the six πN partial waves. Due to the influence of the nuclear environment, those ranges are expected to be different from the πN data and from the results which are derived from fitting light nuclei. However, because of their origin in the πN system, we will take those values as ''reasonable'' if they are not too far away from their corresponding πN values.

(2) For the true absorption we use the form obtained from ^{40}Ca,

$$W_{\rm abs} = \frac{Z\cdot N}{20^2} 515 \frac{\Gamma^2/4}{(E-E_0)^2+\Gamma^2/4}, \tag{3.1}$$

where $E_0 = 215$ MeV, $\Gamma = 77$ MeV, Z and N being the total number of protons and neutrons of the nucleus, respectively. This quantity is to be multiplied by the product of the neutron density times the proton density with each normalized to unit integral probability over the radial variable only.

(3) When the incoming π^+ reaches the surface of the target nucleus its kinetic energy will be decreased roughly by an amount of

$$\Delta E = \frac{Ze^2}{1.4(A)^{1/3}}, \tag{3.2}$$

and hence the optical potential for the π^+ should be evaluated with an appropriately reduced kinetic energy. The values of ΔE are about 14 MeV for ^{208}Pb and 9 MeV for ^{90}Zr. One needs to take into account this kinetic energy reduction in the optical potential calculation, especially, if one deals with low-energy pions. Likewise, when leaving the nuclear surface the kinetic energy of π^- is increased by an amount ΔE, and the same treatment is needed in the calculation of the optical potential.

(4) The single-particle wave functions are important, since (in the present work) they constitute the nuclear density, which determines the distortion of the incoming and outgoing pionic wave, and, in turn, influence the DCX reaction. We calculate the single-particle wave function by solving a Schrödinger equation with a Woods-Saxon type of potential well, the parameters of the well being determined under the condition that the nuclear density has the correct rms proton radius ($\langle r^2\rangle$) and diffuseness, which are listed in the electron scattering data [15]. The charge radii are corrected for the finite size of the proton.

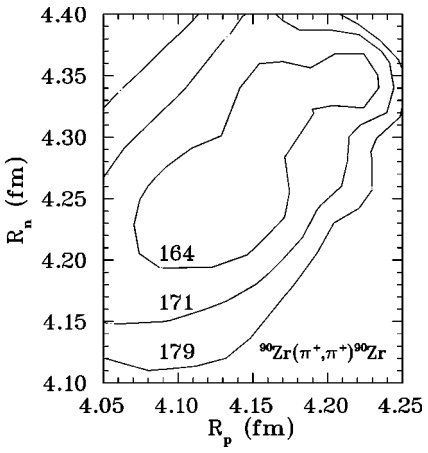

FIG. 1. Contour diagram of the χ^2 on ^{90}Zr.

However, the neutron density remains poorly known. Our strategy is to survey a series of different neutron radii and to find the minimal value of χ^2, as is done in [16]. We create a series of radii for both proton and neutron parts of the density for the nucleus under investigation. For each pair of proton and neutron radii, a minimum is reached for χ^2 with a search on the ranges and multipliers. With those minima we make a contour diagram, then find the lowest minimum χ^2 value and thus determine the proton and neutron radius. Figures 1 and 2 show these contour diagrams for ^{90}Zr and ^{208}Pb, respectively. These diagrams indicate that the radii which give lowest χ^2 values are $R_p = 5.30$ fm, $R_n = 5.60$ fm for ^{208}Pb, and $R_p = 4.17$ fm and $R_n = 4.25$ fm for ^{90}Zr. These proton radii are very close to the corresponding values determined by electron scattering.

The structure of the oscillations of the 162 MeV π^+-^{208}Pb data turns out to be sensitive to the nuclear diffuseness, and a diffuseness of 0.65 fm seems give the best fit.

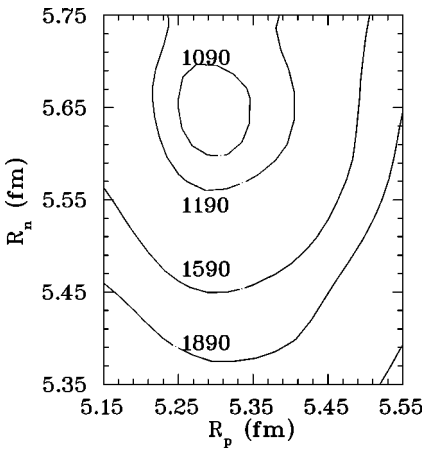

FIG. 2. Contour plot of χ^2 on ^{208}Pb.

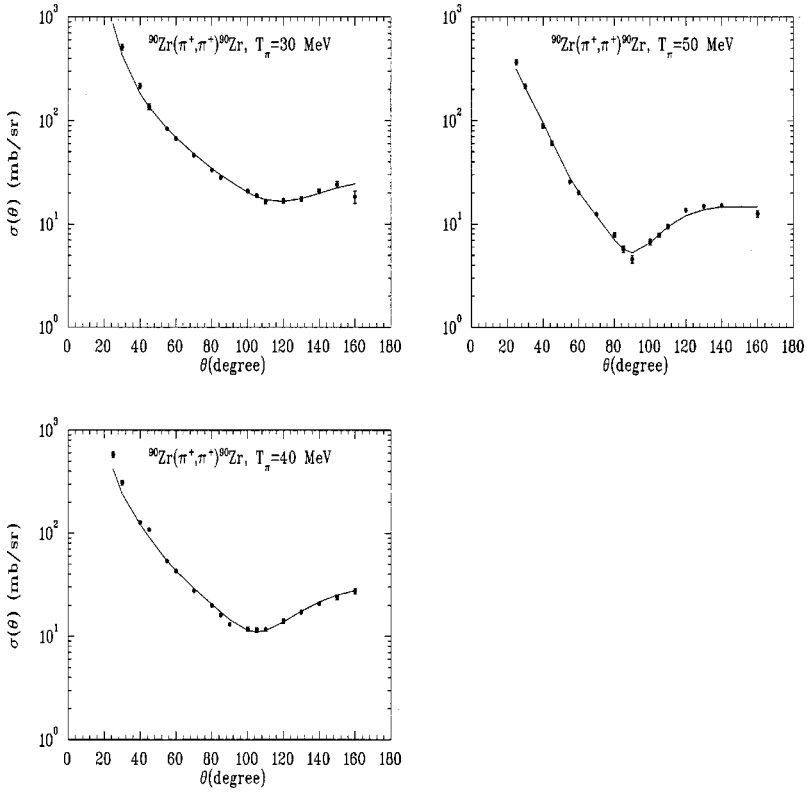

FIG. 3. Pion elastic scattering on ^{90}Zr. The solid line represents the calculation, and points are the experimental data [13,14].

This skin value is also in the vicinity of the electron scattering data [17].

Figures 3 and 4 show the comparison of the experimental and calculated cross sections of the elastic scattering on ^{90}Zr and ^{208}Pb, respectively. The agreement between experiment and calculations is excellent. Table II lists the ranges obtained by fitting the two nuclei. For a comparison we list also the ranges for ^{40}Ca from Ref. [11].

χ^2 for ^{208}Pb is 1083 for 172 data points, and χ^2 of ^{90}Zr is 163 for 52 data points. The ranges from fits to the elastic

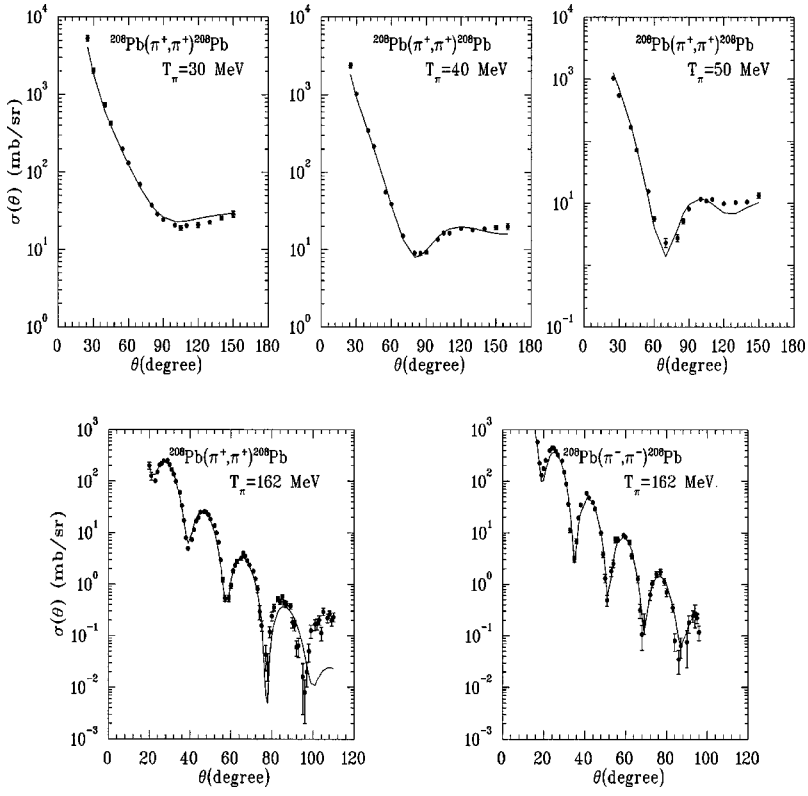

FIG. 4. Pion elastic scattering on ^{208}Pb. The points are the experimental data [12–14].

TABLE II. Ranges from fits to ^{208}Pb and ^{90}Zr.

Partial wave	α_i ^{90}Zr	α_i ^{208}Pb	α_i ^{40}Ca	α_i ^{128,130}Te
S_{11}	404	265	147	300
S_{31}	497	576	556	550
P_{11}	277	202	343	400
P_{31}	210	563	237	400
P_{13}	253	518	173	380
P_{33}	1173	1309	1207	1130

scattering on ^{208}Pb and ^{90}Zr, as is expected, are different from those for ^{40}Ca, but these fitted ranges all seem ''reasonable'' and the two sets of ranges for ^{208}Pb and ^{90}Zr are not very different from each other, even though the two nuclei have a large difference in mass. Due to lack of experimental data on elastic scattering, we are unable to determine the ranges for the Te isotopes through a similar fitting procedure. However, it is reasonable to look for the ranges of Te isotopes in the vicinity of an average of the ranges of ^{208}Pb and ^{90}Zr. In Table II, column 5, we list one such set of ranges for the Te isotopes (see Sec. IV). The normalizations and multiplying factors, as defined in Ref. [11], are shown in Table III.

IV. THE DCX REACTION ON TE ISOTOPES

A. DCX operators in a multi-*j* shell

The extension of the formalism of the DCX reaction from a single-j shell case [1] (AGGK) to a multi-j shell case is straightforward. We use the same notations as AGGK except as stated otherwise. The DCX operator (in coordinate space) is expressed as

$$F_{12}(\boldsymbol{k},\boldsymbol{k}')=[\mathcal{F}_0(\boldsymbol{r}_1,\boldsymbol{r}_2)+\mathcal{F}_1(\boldsymbol{r}_1,\boldsymbol{r}_2)\boldsymbol{\sigma_1}\cdot\mathbf{e_1}\boldsymbol{\sigma_2}\cdot\mathbf{e_2}] *T_-(1)T_-(2), \tag{4.1}$$

where $\mathcal{F}_0$ and $\mathcal{F}_1$ are related to non-spin-flip (NSF) and double-spin-flip (DSF) processes, respectively. The neglect of single-spin-flip (SSF) term is for simplicity and is thought to be a reasonable approximation, since the SSF contribution is zero for the DCX reaction in a shell with same-parity single-particle orbits and for the forward in the plane-wave limit [4]. However, we note that an in-depth investigation of the SSF contribution in heavy nuclei is needed. In the multi-j case it is more convenient to express the DCX operator in pair form:

$$F=\sum_{J,\{j_1j_2\},\{j_3j_4\}} G_{J,\{j_1j_2\},\{j_3j_4\}}(b^\dagger_{j1}b^\dagger_{j2})^J\cdot(\tilde{a}_{j_3}\tilde{a}_{j_4})^J, \tag{4.2}$$

where $\{j_1j_2\}$ means $j_1\geqslant j_2$, and the scalar product is defined as

$$A^J\cdot B^J=\sum_M (-1)^M A^J_M B^J_{-M}. \tag{4.3}$$

The NSF two-body matrix elements consist of direct and exchange terms

$$G^{\rm NSF}_{J,\{j_1j_2\},\{j_3j_4\}}=\frac{2\Omega}{\Delta^2_{1234}}(-1)^{1-j_2-j_4+l_1+l_2-l_3-l_4} \times\sum_L\left\{\begin{Bmatrix} j_1 & j_2 & J\\ j_4 & j_3 & L\end{Bmatrix}Q_L(j_1j_3)Q_L(j_2j_4) \times I^0_L(1234)+(-1)^J{\rm Ex.}\right\}, \tag{4.4}$$

where $Q_L(jj)$ and integral $I^0_L(1234)$ in the direct term stand for

$$Q_L(j_1j_3)=\sqrt{\frac{1}{4\pi}\hat{l}_1\hat{l}_3}(\hat{j}_1\hat{j}_3)^{1/4}\begin{pmatrix} l_1 & l_3 & L\\ 0 & 0 & 0\end{pmatrix}\begin{Bmatrix} l_1 & l_3 & L\\ j_3 & j_1 & 1/2\end{Bmatrix},$$

$$I^0_L(1234)=\int d\boldsymbol{r}_1d\boldsymbol{r}_2\mathcal{F}_0(\boldsymbol{r}_1,\boldsymbol{r}_2)\mathbf{Y}_L(\hat{r}_1)\cdot\mathbf{Y}_L(\hat{r}_2) \times\rho_{l_1l_3}(r_1)\cdot\rho_{l_2l_4}(r_2), \tag{4.5}$$

and

$$\Omega=\{(j_1+1/2)(j_2+1/2)(j_3+1/2)(j_4+1/2)\}^{(1/4)},$$

$$\rho_{l_1l_3}(r_1)=\psi^\pi_{n_1l_1j_1}(r_1)\psi^\nu_{n_3l_3j_3}(r_1),$$

$$\Delta_{1234}=\sqrt{(1+\delta_{j_1j_2})(1+\delta_{j_3j_4})},$$

$$\hat{j}=2j+1. \tag{4.6}$$

The expression for the exchange term (Ex.) is the same as that for direct term except that the orbits j_3 and j_4 are interchanged. The multipolarity L takes even values only when the parities of j_1 and j_3 orbits are the same, whereas it takes odd values only when the parities of j_1 and j_3 are opposite.

The DSF two-body matrix elements consist of

TABLE III. Normalization and scaling factors from fits to ^{208}Pb and ^{90}Zr.

Incoming particle	Energy (MeV)	Normalization ^{208}Pb	Normalization ^{90}Zr
π^+	30	0.81	1.24
π^+	40	0.96	1.39
π^+	50	0.82	1.07
π^+	162	1.25	
π^-	162	1.31	
s multiplier		1.24	1.21
p multiplier		1.22	1.14

$$G^{\mathrm{DSF}}_{J,\{j_1j_2\},\{j_3j_4\}}=\frac{2\Omega}{\Delta^2_{1234}}(-1)^{1-j_2-j_3-l_3-l_4}\times\sum_{L\lambda\lambda'}\left\{\begin{Bmatrix}j_1 & j_2 & J\\ j_4 & j_3 & L\end{Bmatrix}D_{\lambda L}(j_1j_3)D_{\lambda' L}(j_2j_4)\times I^1_L(1234)+(-1)^J\mathrm{Ex.}\right\},\tag{4.7}$$

where

$$D_{\lambda L}(j_1j_3)=\sqrt{2\hat{l}_1\hat{l}_3\hat{\lambda}}(\hat{j}_1\hat{j}_3)^{(1/4)}\begin{pmatrix}l_1 & l_3 & \lambda\\ 0 & 0 & 0\end{pmatrix}\times\begin{Bmatrix}\lambda & 1 & L\\ l_1 & \frac{1}{2} & j_1\\ l_3 & \frac{1}{2} & j_3\end{Bmatrix},$$

$$I^1_L(1234)=\int d\boldsymbol{r}_1d\boldsymbol{r}_2\mathcal{F}_1(\boldsymbol{r}_1,\boldsymbol{r}_2)\mathbf{Y}_{\lambda L}(\hat{r}_1)\cdot\mathbf{Y}_{\lambda' L}(\hat{r}_2)\times\rho_{l_1l_3}(r_1)\rho_{l_2l_4}(r_2),\tag{4.8}$$

in which the vector spherical harmonic $\mathbf{Y}_{\lambda L}(\hat{\mathbf{r}}_1)$ is defined as

$$\mathbf{Y}_{\lambda L}(\hat{\mathbf{r}}_1)=[\mathbf{Y}_\lambda(\hat{\mathbf{r}}_1)\mathbf{Y}_1(\hat{\mathbf{e}}_1)]^L.\tag{4.9}$$

The multipolarity L takes odd values only when the parities of j_1 and j_3 orbits are the same, whereas it takes even values only when the parities of j_1 and j_3 are opposite.

In multipole form the DCX operator looks the same as in the AGGK paper,

$$F=\Omega\sum_{L,\{j_1j_2\},\{j_3j_4\}}F_{L\{j_1j_2\},\{j_3j_4\}}(\boldsymbol{k},\boldsymbol{k}')\times(b^\dagger_{j_1}\tilde{a}_{j_3})^L\cdot(b^\dagger_{j_2}\tilde{a}_{j_4})^L/(2L+1),\tag{4.10}$$

however, the actual expression of the matrix elements F_L is more complex. The matrix elements F_L and G_J can be transformed to one another according to the following formulas:

$$G_{J,\{j_1j_2\}\{j_3j_4\}}=\Omega(-1)^{1-j_2-j_3}\sum_L\begin{Bmatrix}j_1 & j_3 & L\\ j_4 & j_2 & J\end{Bmatrix}\times F_{L,\{j_1j_2\},\{j_3j_4\}},\tag{4.11}$$

$$F_{L,\{j_1j_2\}\{j_3j_4\}}=\frac{1}{\Omega}(-1)^{1+j_2+j_3}\sum_J\begin{Bmatrix}j_1 & j_3 & L\\ j_4 & j_2 & J\end{Bmatrix}\times G_{J,\{j_1j_2\}\{j_3j_4\}}\hat{J}\hat{L}.\tag{4.12}$$

As a verification of these formulas, one can let all j's be equal and the formulas of F_L in the AGGK paper are reproduced.

We are interested in calculating the DIAS and g.s. transitions which involve only the zeroth component of the DCX operator. In the generalized seniority scheme the amplitude of DIAS transition can be calculated as follows [4]:

$$\langle\hat{F}\rangle_{\mathrm{DIAS}'}=\mathcal{N}_d^{-1}\sum_{j,k,J}\sum_{\{j_1j_2\},\{j_3j_4\}}(-1)^{1+J}G_{J,\{j_1j_2\},\{j_3j_4\}}\times\langle S_\pi|[(\tilde{b}_j\tilde{b}_k)^{(J)}(b^\dagger_{j_1}b^\dagger_{j_2})^{(J)}]^{(0)}|S_\pi\rangle\times\langle S^{N_\nu}_\nu|[(a^\dagger_ja^\dagger_k)^{(J)}(\tilde{a}_{j_3}\tilde{a}_{j_4})^{(J)}]^{(0)}|S^{N_\nu}_\nu\rangle,\tag{4.13}$$

where $\mathcal{N}_d^{-1}$ is the normalization of the double analog state of Xe isotopes, and

$$\langle S^{N_\nu}_\nu|[(a^\dagger_ja^\dagger_k)^{(J)}(\tilde{a}_{j_3}\tilde{a}_{j_4})^{(J)}]^{(0)}|S^{N_\nu}_\nu\rangle=\begin{cases}-\sqrt{2J+1}(\langle S^{N_\nu}_\nu|(a^\dagger_ja^\dagger_k)^{(J)}_0|S^{N_\nu-2}_\nu(a_ja_k)^{(J)}_0\rangle)^2\delta_{jj_3}\delta_{kj_4} & J>0\\ -\langle S^{N_\nu}_\nu|(a^\dagger_ja^\dagger_j)^{(0)}(a_{j_3}a_{j_3})^{(0)}|S^{N_\nu}_\nu\rangle\delta_{jk}\delta_{j_3j_4} & J=0,\end{cases}\tag{4.14}$$

which can be calculated easily with the pair structure coefficients $\alpha_{\rho j}$ (listed in Table I).

The amplitude of the g.s. transition are much simpler than that of DIAS [4]:

$$\langle\hat{F}\rangle^0_{\mathrm{g.s.}}=\langle\mathrm{Xe,g.s.}|\hat{F}|\mathrm{Te,g.s.}\rangle\simeq\langle S^2_\pi S_\nu{}^{N_\nu-1}|\hat{F}|S_\pi S_\nu{}^{N_\nu}\rangle=\sum_{j_1,j_3}G_{0,\{j_1j_1\},\{j_3j_3\}}\langle S^2_\pi|(b^\dagger_{j_1}b^\dagger_{j_1})^{(0)}|S_\pi\rangle\times\langle S^{N_\nu-1}_\nu|(\tilde{a}_{j_3}\tilde{a}_{j_3})^{(0)}|S^{N_\nu}_\nu\rangle.\tag{4.15}$$

From the discussion in Ref. [4] the only relevant configurations are

$$\{j_aj_a\}\{j_bj_b\}\quad\text{or}\quad\{j_aj_b\}\{j_aj_b\},\tag{4.16}$$

which greatly simplifies the calculations.

B. Angular distribution of DCX cross section at $E_{\mathrm{lab}}=48$ MeV

Due to their special importance in both DCX reaction and double β decay, the isotopes ^{128}Te and ^{130}Te have attracted attention from nuclear physicists [3,4].

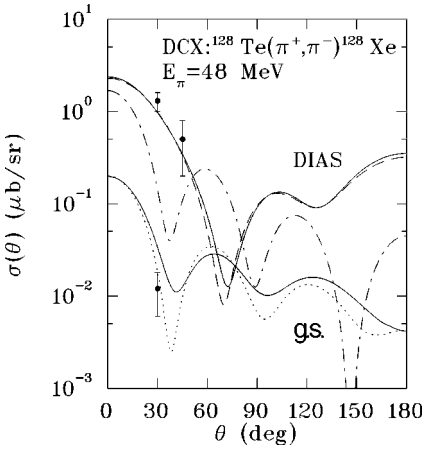

FIG. 5. Angular distribution of the DCX reaction on ^{128}Te. The curves labeled DIAS and g.s. represent the double isobaric analog state transition and the ground-state transition, respectively. Two types of nuclear wave function are used: generalized seniority model and seniority model. See the text for a more detailed explanation of the correspondences. The experimental data are taken from [18].

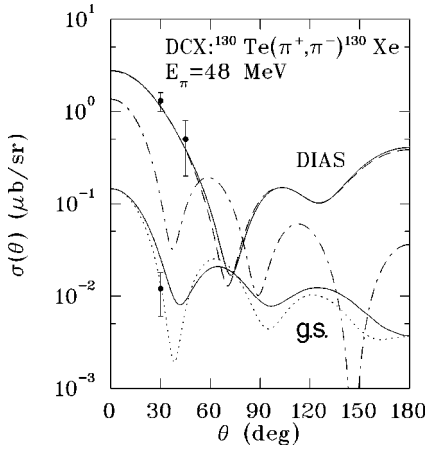

FIG. 6. Angular distribution of the DCX reaction on ^{130}Te. See Fig. 5 for an explanation of the meaning of the curves and points.

The valence shell protons and neutrons are in the same shell consisting of the following orbits: $g7/2$, $d5/2$, $d3/2$, $s1/2$, and $h11/2$. Since they are near-spherical nuclei, the application of generalized seniority model is appropriate [9]. In the generalized seniority model the number of nucleon pairs with nonzero contribution to the DCX amplitude is limited to 35, Eq. (4.16).

The ranges α_i play an important role in double charge exchange reaction as well as in elastic scattering. It is preferable that one calculates the DCX reaction for Te isotopes with the ranges which are determined in fitting elastic scattering. However, since there are no such elastic-scattering data available, we instead look for a set of ranges, which reproduce well the DCX data of Te isotopes and which are in the vicinity of the averaged ranges of ^{90}Zr and ^{208}Pb. Since the two sets of ranges of ^{90}Zr and ^{208}Pb are very close despite the big difference in mass between the two nuclei, one has reason to expect that Te isotopes, with an intermediate mass, should have ranges not too far away from the ranges of ^{90}Zr and ^{208}Pb.

We list such a set of ranges for Te in column 5 of Table II. The angular distribution of the DCX cross section on Te isotopes is calculated at the pion lab energy equal to 48 MeV. Figures 5 and 6 show a comparison between experimental data [18] and calculations with this set of ranges for ^{128}Te and ^{130}Te, respectively. Two types of nuclear wave function are used in the calculation: the generalized seniority model wave function (realistic) and the seniority model wave function. The upper solid line and long-dashed line represent the DIAS transition with realistic and seniority wave functions, respectively. The lower solid line and dot-dashed line are the g.s. transition with realistic and seniority wave functions, respectively. The two-orders-of-magnitude difference between DIAS and g.s. transition data at 30 degrees is well reproduced. It is found that the DCX cross section is very sensitive to the P_{33} range. Therefore, one may be more or less confident about the choice of P_{33} range (1130 MeV/c), although elastic-scattering fitting is not done. We note that the results in Figs. 5 and 6 are only preliminary, since the elastic scattering is not fitted and the DCX data are so scarce.

As is pointed out in Ref. [4] that the general seniority wave function, Eq. (2.1), is not an isospin pure state. It has a mixing of higher isospin component (the probability is less than 2%), which we call ''spurious'' isospin mixing. The amplitude of this mixing, δ, can be calculated as follows [4]:

$$\delta = \mathcal{N}_d^{-1} \langle S_\pi^2 S^{N_\nu - 1} | T_- T_- | S_\pi S^{N_\nu} \rangle. \tag{4.17}$$

To remove this mixing, the following subtraction needs to be done [4]

$$\langle \hat{F} \rangle_{\text{g.s.}} = \langle \hat{F} \rangle^0_{\text{g.s.}} - \delta \langle \hat{F} \rangle_{\text{DIAS}}, \tag{4.18}$$

where $\langle \hat{F} \rangle^0$ is the DCX matrix elements before removing this spurious mixing. In Figs. 5 and 6 the dotted line represents the g.s. transition with the realistic seniority model after removing this mixing. It seems that, while in general this correction is not big, it is important for some angles.

It is interesting to note that while two type of nuclear wave functions produce very different g.s. transition rates, the DIAS transition rates are very close. It confirms the same conclusion in a previous study in the plane-wave limit [4]. One may roughly state that the DIAS rates depend mainly on the two-step sequential process, whereas the g.s. rates have more to do with nuclear structure.

C. Energy dependence of the DCX cross section

In the studies of DCX reaction for light nuclei at low energies, a peak was observed in the vicinity of $T_\pi = 40$ MeV. This peak has been understood as the consequences of the pion propagation in the conventional two-step sequential process, which includes not only the distortion of π^+ and π^- but also the distorted Green function of π^0.

We calculate the energy dependence of the pionic DCX reaction on ^{128}Te (Fig. 7) by using the set of ranges listed in Table II. A peak remains at around 40 MeV, however, the

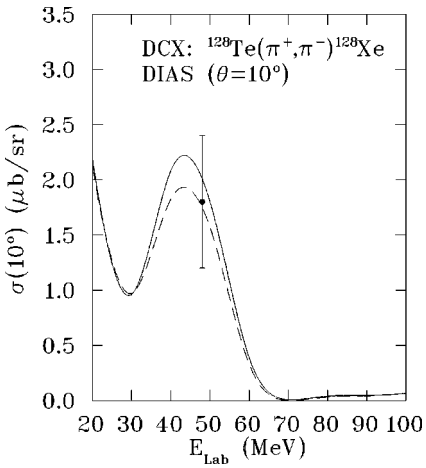

FIG. 7. Energy dependence of the DCX cross section for ^{128}Te. The rates are given for DIAS transition in the two cases: NSF (long dashed line) and NSF+DSF (full line), respectively. The generalized seniority model wave function is employed for both cases. NSF and DSF stand for non-spin-flip and double-spin-flip, respectively. The only experimental data point is taken from [18], which is extrapolated to the forward angle transition.

shape of this peak depends very much on the set of ranges used. Therefore, the results in Fig. 7 can be viewed as only tentative. To further test the theory, more experiments are needed.

V. CONCLUSION AND DISCUSSION

The application of generalized seniority model to the study of DCX reactions is motivated by the success of this model in the study of a series of medium and heavy nuclei [9]. However, when dealing with DCX reactions one has to be more careful about the consequences of neglecting higher seniority components.

First we consider the role of higher seniority components in the calculation of the optical potentials. One could improve the approximation by including a mixture of a small seniority-four component (denoted as $|\nu=4\rangle$) as follows:

$$|\text{g.s.}\rangle = |S_\pi^{N_\pi} S_\nu^{N_\nu}\rangle + \eta |(D_\pi D_\nu)^0 S_\pi^{N_\pi - 1} S_\nu^{N_\nu - 1}\rangle \equiv |\nu=0\rangle + \eta |\nu=4\rangle, \tag{5.1}$$

where $|\nu=0\rangle$ denotes the dominant component [Eq. (2.1)], and one assumes that $\eta \ll 1$. In the generalized seniority model the states with seniority higher than zero are not well defined. Here $|\nu=4\rangle$ is understood as a seniority four state in the sense that four nucleons are not forming angular momentum zero pairs. The optical potential produced by the valence nucleons is

$$\langle \boldsymbol{k}' | V_{\text{opt}}(E) | \boldsymbol{k} \rangle = \langle \text{g.s.} | \hat{V} | \text{g.s.} \rangle = \langle \nu=0 | \hat{V} | \nu=0 \rangle + 2\,\eta \langle \nu=0 | \hat{V} | \nu=4 \rangle + \eta^2 \langle \nu=4 | \hat{V} | \nu=4 \rangle. \tag{5.2}$$

The off-diagonal part in Eq. (2.5) (with $j_1 \neq j_2$) can change seniority at most by two, therefore, the second term in Eq. (5.2) will vanish, and the only correction brought about by the mixture of $|\nu=4\rangle$ is the last term in the right-hand side. According to a phenomenological calculation in Ref. [19], the value of η for the near-spherical nuclei, such as ^{128,130}Te ^{128,130}Xe, is less than 0.2 so that the η^2 term is only about 0.04, which is negligible.

Second, we discuss the importance of higher seniority components to the DCX amplitudes. As was demonstrated in this work and in a previous work [4], the DIAS transition mainly depends on the two-body sequential process, π scattering and π wave distortion, in which the optical potentials are of crucial importance. The dependence of DCX amplitude on the pair coefficients of the generalized seniority wave function is only minor. Therefore, one has good reason to assume that the mixing of a small component $|\nu=4\rangle$ will not bring about significant changes to the DIAS amplitude. However, for the g.s. transition the mixing of higher seniority components may have a considerable effect. It is an involved task to study the nuclear structure in a space with all the seniority four components which we leave to a future investigation.

The motivation of this work was to investigate the DCX reaction on heavy nuclei such as Te isotopes, based on a sequential scattering mechanism plus realistic nuclear wave function and pionic distortions. For this purpose the optical potential is of crucial importance, therefore, the fine tuning via fitting elastic scattering is indispensable. The fitting of the elastic scattering on ^{208}Pb and ^{90}Zr reproduce the experimental data very well, which shows that the extension of the model of [6,7] is applicable to more complex shells.

For a quantitative investigation on Te isotopes one would need to test the optical potential and to determine the parameters also via fitting elastic scattering. However, this is not possible due to the lack of data. Instead we took the average of the parameters of ^{208}Pb and ^{90}Zr as guidance in determining ranges for Te. This makes our calculation and the comparison to data less quantitative. However, the reproduction of (rare) DCX data on Te isotopes with a set of ranges in the vicinity of the ranges of ^{90}Zr and ^{208}Pb is, at least, an encouraging sign of the adequacy of the use of the two-step sequential process and the generalized seniority model. To further understand the double charge exchange reaction more experimental data are needed, especially for heavy nuclei.

The nuclei ^{128,130}Te have been a focus of combined studies of double charge exchange reaction and double beta decay, since both reactions turn two neutrons into protons. It is natural to demand that any successful nuclear model should be able to explain the two reactions at the same time.

The pnQRPA gained success in reproducing the double beta decay by adjusting the particle-particle coupling strength g_{pp} [20]. However, in dealing with ^{100}Mo the method encountered a fatal problem that is the collapse of ground state, which is due to the violation of Pauli principle. This collapse is repaired by introducing a numerical procedure called ''renormalization'' [21]. However, the physics behind the violation of Pauli principle and the renormalization procedure needs to be further explored.

The generalized seniority model, as is shown in this work, explains the elastic scattering and double charge exchange in a consistent manner, but it fails to reproduce the double beta decay data [22]: the calculated matrix element $\mathcal{M}_{\mathrm{GT}}$ is about seven times as big as the experimental value; and all other shell-model-related models, such as the weak-coupling model [23] and interacting boson model [19], have the same problem. This discrepancy presents a serious challenge to the generalized seniority model.

In Ref. [22] a schematic analysis of the double β decay revealed that the generalized seniority model (as well as other shell-model related approaches) employs a wave function which has a small mixing of higher isospin component. We call this a ''spurious'' mixing since it is caused not by underline physics but by the special choice of the wave function for the ground state. By removing this spurious mixing the matrix element $\mathcal{M}_{\mathrm{GT}}$ is reduced by 10%, which is not enough to explain data but is in the right direction. A further consideration of the isospin involves the ''physical'' mixing of the isospin (caused by the Coulomb force and the charge dependent and charge asymmetric nuclear interactions) in the ground states of the isotopes Te and the intermediate isotopes *I*. Although the probability of this mixing is very small, it can contribute to the double β decay significantly, since the matrix element of the Fermi operator is much larger than its Gamow-Teller counterpart. Another phenomenon which could be related to our understanding of double β decay is the single β decay, since the ''hindrance'' factor in single β decay is not yet well understood. The hindrance factor is a number needed to modify the single β decay operators in order to reproduce data; the factor is about 0.8 for ds shell nuclei [24] and about 0.3 for medium-weight nuclei [25]. The hope of understanding double β decay based on the generalized seniority model might exist in a joint study of the single β decay and double β decay with proper handling of the isospin.

ACKNOWLEDGMENTS

The work was supported by Colciencias and University of Antioquia, Colombia, and by the U.S. Department of Energy. H.C.W. acknowledges the hospitality of the Physics Department, New Mexico State University, during his visits to the institution.

[1] N. Auerbach, W. R. Gibbs, N. Ginocchio, and W. B. Kaufmann, Phys. Rev. C **38**, 1277 (1988).
[2] H. Clement, Prog. Part. Nucl. Phys. **29**, 175 (1992).
[3] W. A. Kaminski and A. Faessler, Nucl. Phys. **A529**, 605 (1991).
[4] H. C. Wu, J. Ginocchio, A. Dieperink, and O. Scholten, Phys. Rev. C **54**, 1208 (1996).
[5] M. Nuseirat, M. K. Lodhi, M. O. El-Ghossain, W. R. Gibbs, and W. B. Kaufmann, Phys. Rev. C **58**, 2292 (1998).
[6] H. Garcilazo and W. R. Gibbs, Nucl. Phys. **A356**, 284 (1981).
[7] W. B. Kaufmann and W. R. Gibbs, Phys. Rev. C **28**, 1286 (1983).
[8] I. Talmi, Nucl. Phys. **A172**, 1 (1971).
[9] O. Scholten, Phys. Rev. C **28**, 1783 (1983); O. Scholten and H. Kruse, Phys. Lett. **125B**, 113 (1983).
[10] S. Pittel, P. D. Duval, and B. R. Barrett, Ann. Phys. (N.Y.) **144**, 168 (1982).
[11] M. Nuseirat, M. K. Lodhi, and W. R. Gibbs, Phys. Rev. C **58**, 314 (1998).
[12] M. J. Devereux, Ph.D. thesis, New Mexico State University, 1979.
[13] B. M. Preedom *et al.*, Phys. Rev. C **23**, 1134 (1981).
[14] M. Blecher *et al.*, Phys. Rev. C **20**, 1884 (1979).
[15] H. de Vries, C. W. de Jager, and C. de Vries, At. Data Nucl. Data Tables **36**, 495 (1987); G. Friche *et al.*, *ibid.* **60**, 177 (1995).
[16] W. R. Gibbs and J. P. Dedonder, Phys. Rev. C **46**, 1825 (1992).
[17] W. F. Hornyak, *Nuclear Structure* (Academic, New York, 1975).
[18] K. Föhl *et al.*, Phys. Rev. C **53**, R2033 (1996).
[19] O. Scholten and Z. R. Yu, Phys. Lett. **161B**, 13 (1985).
[20] O. Civitarese, A. Faessler, and T. Tomoda, Phys. Lett. B **194**, 11 (1987).
[21] T. Toivanen and J. Suhonen, Phys. Rev. Lett. **75**, 410 (1995).
[22] H. C. Wu, A. Dieperink, M. J. Paez, W. A. Ponce, and O. Scholten, Proceedings of the Conference on Nuclear Data in Science and Technology, edited by G. Reffo *et al.*, Trieste, 1997, p. 336.
[23] W. C. Haxton, G. J. Stephenson, and D. Strottman, Phys. Rev. D **25**, 2360 (1982).
[24] B. A. Brown and B. H. Widenthal, At. Data Nucl. Data Tables **33**, 347 (1985).
[25] F. Dellagiacoma and F. Iachello, Phys. Lett. B **218**, 399 (1989).